Geophysical Research Letters

RESEARCH LETTER
10.1029/2021GL096365

Key Points:

- ENSO impact on the tropical Atlantic precipitation migrates meridionally along with the local seasonal cycle phase
- A robust year-round relationship can be established between ENSO and tropical Atlantic precipitation by involving the seasonal cycle
- The extended perspective on ENSO's impact enhances prospects for seasonal climate prediction over the tropical Atlantic

Supporting Information:

Supporting Information may be found in the online version of this article.

Correspondence to:

W. Zhang,
zhangwj@nuist.edu.cn

Citation:

Jiang, F., Zhang, W., Jin, F.-F., & Stuecker, M. F. (2021). Meridional migration of ENSO impact on tropical Atlantic precipitation controlled by the seasonal cycle. *Geophysical Research Letters*, *48*, e2021GL096365. https://doi.org/10.1029/2021GL096365

Received 29 SEP 2021
Accepted 26 NOV 2021

Meridional Migration of ENSO Impact on Tropical Atlantic Precipitation Controlled by the Seasonal Cycle

Feng Jiang[1], Wenjun Zhang[1], Fei-Fei Jin[2], and Malte F. Stuecker[3]

[1]Key Laboratory of Meteorological Disaster of Ministry of Education (KLME), Nanjing University of Information Science and Technology, Nanjing, China, [2]Department of Atmospheric Sciences, School of Ocean and Earth Science and Technology (SOEST), University of Hawai'i at Mānoa, Honolulu, HI, USA, [3]Department of Oceanography & International Pacific Research Center (IPRC), School of Ocean and Earth Science and Technology (SOEST), University of Hawai'i at Mānoa, Honolulu, HI, USA

Abstract Previous studies suggest that the El Niño–Southern Oscillation (ENSO) impact on tropical Atlantic climate variability shows strong seasonal preference, manifesting itself primarily in the decaying boreal spring season. However, here we show that a robust ENSO signal in tropical Atlantic precipitation anomalies can be detected throughout ENSO's whole lifecycle. We find that the ENSO impact on the tropical Atlantic precipitation migrates meridionally, following the seasonal migration of the Atlantic Intertropical Convergence Zone (ITCZ). Taking into account the modulation of the local seasonal cycle, the full spatiotemporal characteristics of ENSO's impact on tropical Atlantic precipitation are uncovered. Furthermore, we demonstrate that climate models can simulate the modulation of ENSO-related precipitation over the tropical Atlantic by the local seasonal cycle despite the substantial mean state model bias in the Atlantic ITCZ. This extended perspective on ENSO's impact on tropical Atlantic climate variability enhances prospects for skillful year-round regional climate prediction.

Plain Language Summary El Niño–Southern Oscillation (ENSO) provides the primary source of predictability for the tropical Atlantic precipitation on interannual time scales. In most previous studies, a strong seasonal preference in the ENSO teleconnection to the Atlantic was identified. We here demonstrate that ENSO's impact on tropical Atlantic precipitation can be detected from ENSO developing to decaying phases, which is strongly modulated by the local seasonal cycle regarding its meridional migration. On this basis, we establish a robust year-round statistical relationship between ENSO and tropical Atlantic precipitation by involving the local seasonal cycle. This observed modulation of the local seasonal cycle on ENSO's impact can also be simulated in the state-of-the-art climate models. It is suggested that the realistic representation of the Atlantic seasonal cycle, as well as the improved ENSO prediction, could directly translate into enhanced prediction skill over the tropical Atlantic sector.

1. Introduction

The El Niño–Southern Oscillation (ENSO) is the dominant air–sea coupled mode of interannual climate variability on Earth (e.g., Bjerknes, 1969; Jin, 1997; Neelin et al., 1998; Philander, 1990; Rasmusson & Carpenter, 1982; Wyrtki, 1975). While originated in the tropical Pacific, ENSO has consequences felt worldwide via far-reach teleconnections, such as the Pacific–North American (PNA) teleconnection pattern (e.g., Horel & Wallace, 1981; McPhaden et al., 2006; Ropelewski & Halpert, 1987; Wallace et al., 1998). Within the tropics, ENSO can induce pronounced climate fluctuations in the tropical Indian and Atlantic Oceans by altering the Walker Circulation (e.g., Cai et al., 2019; Enfield & Mayer, 1997; Klein et al., 1999; Saravanan & Chang, 2000; Yun et al., 2021). Numerous studies have explored the crucial role of ENSO in shaping Indian Ocean climate variability in consideration of the actively interconnected climate system in the Indo-Pacific region (e.g., Behera et al., 2006; Reason et al., 2000; Stuecker et al., 2017; Yang et al., 2007). Simultaneously, ENSO teleconnection to the Atlantic is also recognized to provide the fundamental source of seasonal predictability for tropical Atlantic climate variability (e.g., Covey & Hastenrath, 1978; Enfield & Mayer, 1997; Giannini et al., 2001; Kushnir et al., 2006; Nobre & Shukla, 1996; Saravanan & Chang, 2000).

It has been long established that the El Niño-related upward atmospheric motion anomalies can directly induce an anomalous downward atmospheric motion over the tropical Atlantic Ocean based on both observational analyses

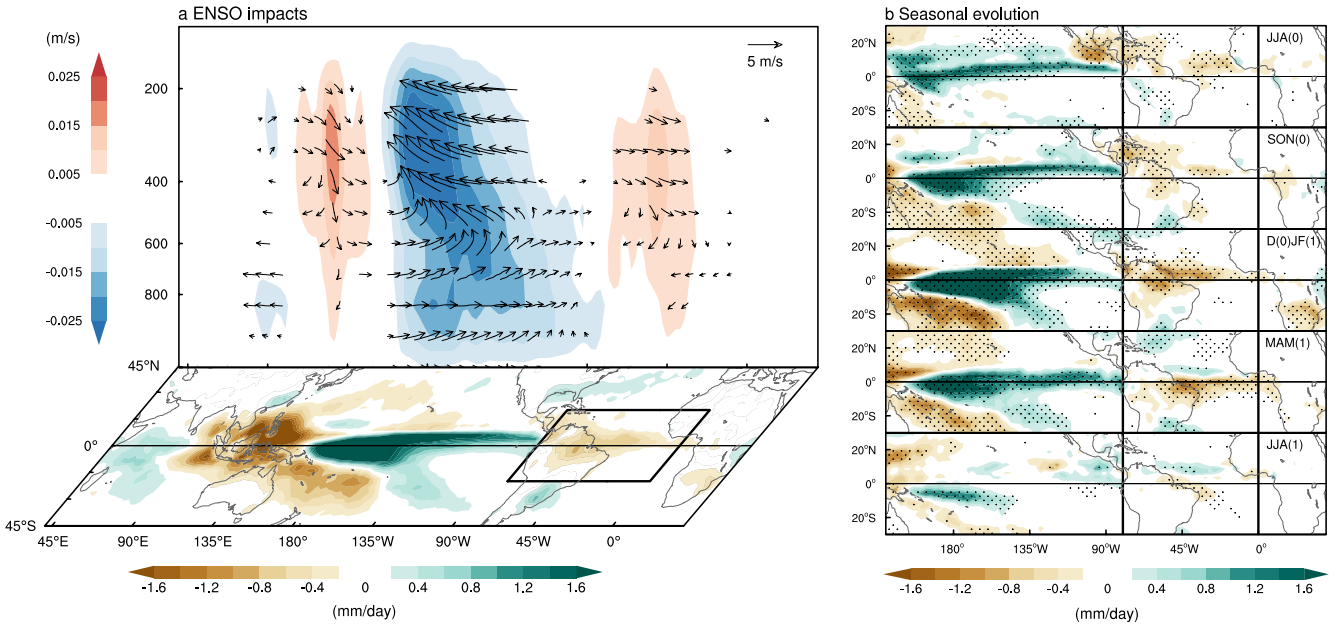

Figure 1. (a) Zonal wind and vertical velocity anomalies on the equator (vector; m/s) and precipitation anomalies (shading; mm/day) regressed upon the monthly Niño3.4 index. The vertical velocity anomalies are multiplied by a factor of −200 for the vectors and also shown in shading. Vectors smaller than 0.5 m/s are omitted. The black box indicates the tropical Atlantic region (20°S–20°N, 0°W–80°W). (b) Precipitation anomalies (shading; mm/day) in JJA(0), SON(0), D(0)JF(1), MAM(1), and JJA(1) regressed upon the D(0)JF(1) Niño3.4 index. Numerals "0" and "1" indicate El Niño–Southern Oscillation (ENSO) developing and decaying years, respectively. Dots in (b) indicate regression coefficients that are statistically significant at the 95% confidence level.

and numerical experiments (e.g., Chiang et al., 2002; Saravanan & Chang, 2000; Sasaki et al., 2015). On interannual time scales, ENSO is widely regarded as one of the most prominent remote forcings of tropical Atlantic precipitation. Generally, warm and cold ENSO episodes correspond to reduced and enhanced precipitation over much of the tropical Atlantic, respectively (Chiang et al., 2002; Giannini et al., 2001; Sasaki et al., 2015). Most previous studies concerning the ENSO impacts on the Atlantic climate variability have been primarily focused on the boreal spring season, identifying a strong seasonal preference in the ENSO teleconnection to the tropical Atlantic Ocean (e.g., Chiang et al., 2002; García-Serrano et al., 2017; Giannini et al., 2001; Münnich & Neelin, 2005; Sasaki et al., 2015; S. P. Xie & Carton, 2004). The seasonal preference stems largely from the lagged behavior of the North Tropical Atlantic (NTA) sea surface temperature (SST) response to ENSO, which can be interpreted as resulting from the seasonality of the extratropical PNA teleconnection (Kim et al., 2018; Livezey et al., 1997; Wang & Fu, 2000) or the local SST adjustment time scale (Alexander et al., 2002; Chang et al., 2006; Lintner & Chiang, 2007). Less apparent seasonal preference, however, would be expected for ENSO's impact on tropical Atlantic precipitation since the modulation of tropical general circulation appears operative throughout the ENSO cycle. Actually, an ENSO signal can be detected in precipitation anomalies within the tropical Atlantic region during different seasons as shown in some early findings, despite discrepancies among different studies (Alexander & Scott, 2002; Dai & Wigley, 2000; Enfield & Alfaro, 1999; Giannini et al., 2001; see also Figure 1b). Particularly, the strength and location of tropical Atlantic precipitation anomalies associated with ENSO show large variations across seasons.

The prevailing notion that is focused on the spring season is not sufficient and a more extended perspective is therefore needed in appreciating the full impact of ENSO on tropical Atlantic precipitation. In this study, we demonstrate that the impact of ENSO on tropical Atlantic precipitation is strongly modulated by the seasonal cycle, characterized with prominent seasonal meridional displacement following the Atlantic Intertropical Convergence Zone (ITCZ) migration. On this basis, we establish a robust year-round relationship between ENSO and tropical Atlantic precipitation by involving the modulation of the seasonal cycle. An implication is that potential predictability of the Atlantic Ocean sector provided by ENSO is larger than previously recognized.

2. Data and Methods

2.1. Data Sets

The utilized SST data set in this study is the global sea ice and SST analyses from the Hadley Centre (HadISST version 1.1) provided by the Met Office Hadley Centre (Rayner et al., 2003). The precipitation data set is the global precipitation product from the Climate Prediction Center (CPC) Merged Analysis of Precipitation (CMAP; P. Xie & Arkin, 1996). The atmospheric circulation data sets, including horizontal wind and vertical velocity, are the National Centers for the Environmental Prediction–National Center for the Atmospheric Research (NCEP–NCAR) reanalysis (Kalnay et al., 1996). The horizonal resolution is $1° \times 1°$ for the SST data set and $2.5° \times 2.5°$ for the precipitation and circulation data sets.

Monthly SST and precipitation output of the preindustrial control (pi-control) simulations from 50 available Coupled Model Intercomparison Project Phase 6 (CMIP6) climate models are utilized (Table S1). Only one ensemble member for each model is used, mostly r1i1p1f1 with selected models using r1i1p1f2 based on the availability. The last 100 years of model simulations are used for the analysis. All the model data sets were bilinearly interpolated onto a regular $1° \times 1°$ grid.

2.2. Methods

The observational analyses covered the period from 1979 to 2020, and anomalies for all variables were computed by removing the monthly mean climatology (1979–2020). The linear trends were removed from all data sets to avoid possible influences associated with global warming. The monthly data were stratified into four seasons when exploring the seasonally varying ENSO influence: March–May (MAM), June–August (JJA), September–November (SON), and December–February (DJF). All statistical significance tests were performed using the two-tailed Student's t test.

ENSO events were defined according to the CPC's definition based on a threshold of $\pm 0.5°C$ of the Niño3.4 index (SST anomalies averaged over 5°S–5°N, 120°W–170°W) for five consecutive months for the observation. Following this criterion, 14 El Niño events (1979, 1982, 1986, 1987, 1991, 1994, 1997, 2002, 2004, 2006, 2009, 2014, 2015, and 2018) and 14 La Niña events (1983, 1984, 1985, 1988, 1998, 1999, 2000, 2005, 2007, 2008, 2010, 2011, 2016, and 2017) were identified. For the model data, ENSO events were selected when the averaged Niño3.4 index in boreal winter exceeds 0.7 standard deviation. We used the difference between El Niño- and La Niña-related precipitation anomalies to characterize the ENSO impacts, since the La Niña impact on tropical Atlantic precipitation is roughly similar in its spatial structure to that of El Niño with anomalies of opposite sign.

The Atlantic ITCZ latitude ($\bar{L}$) for each month (t) was calculated as the zonally averaged precipitation-weighted mean latitude:

$$\bar{L}(t) = \frac{\int_{-20}^{20} Pr(L,t) * L dL}{\int_{-20}^{20} Pr(L,t) dL}, \quad (1)$$

where Pr denotes the zonally averaged precipitation over the tropical Atlantic (0°W–80°W) and L denotes latitude in ° (Gadgil & Guruprasad, 1990; Waliser & Gautier, 1993).

3. Full Extent of the ENSO Impact on Tropical Atlantic Precipitation

We in Figure 1 display the full spatiotemporal characteristics of ENSO's impact on tropical Atlantic precipitation following an ENSO lifecycle from its developing to decaying phases (Giannini et al., 2001; Rasmusson & Carpenter, 1982). Overall, negative precipitation anomalies are observed over the tropical Atlantic during El Niño events due to the anomalous Walker Circulation (Figure 1a). We emphasize that the ENSO-related precipitation anomalies over the tropical Atlantic Ocean exhibit a clear seasonal variation with the main part being in the most northern part during the developing boreal autumn season, shifting to the most southern part in the decaying boreal spring (Figure 1b). This acts in concert with the seasonal north-south ITCZ migration (Figures S1 and 2a).

The Atlantic ITCZ, manifested by a narrow band of heavy precipitation where the trade winds converge, has a pronounced north-south asymmetry (Figure S1a). In general, the ITCZ is located over the tropical ocean and extends

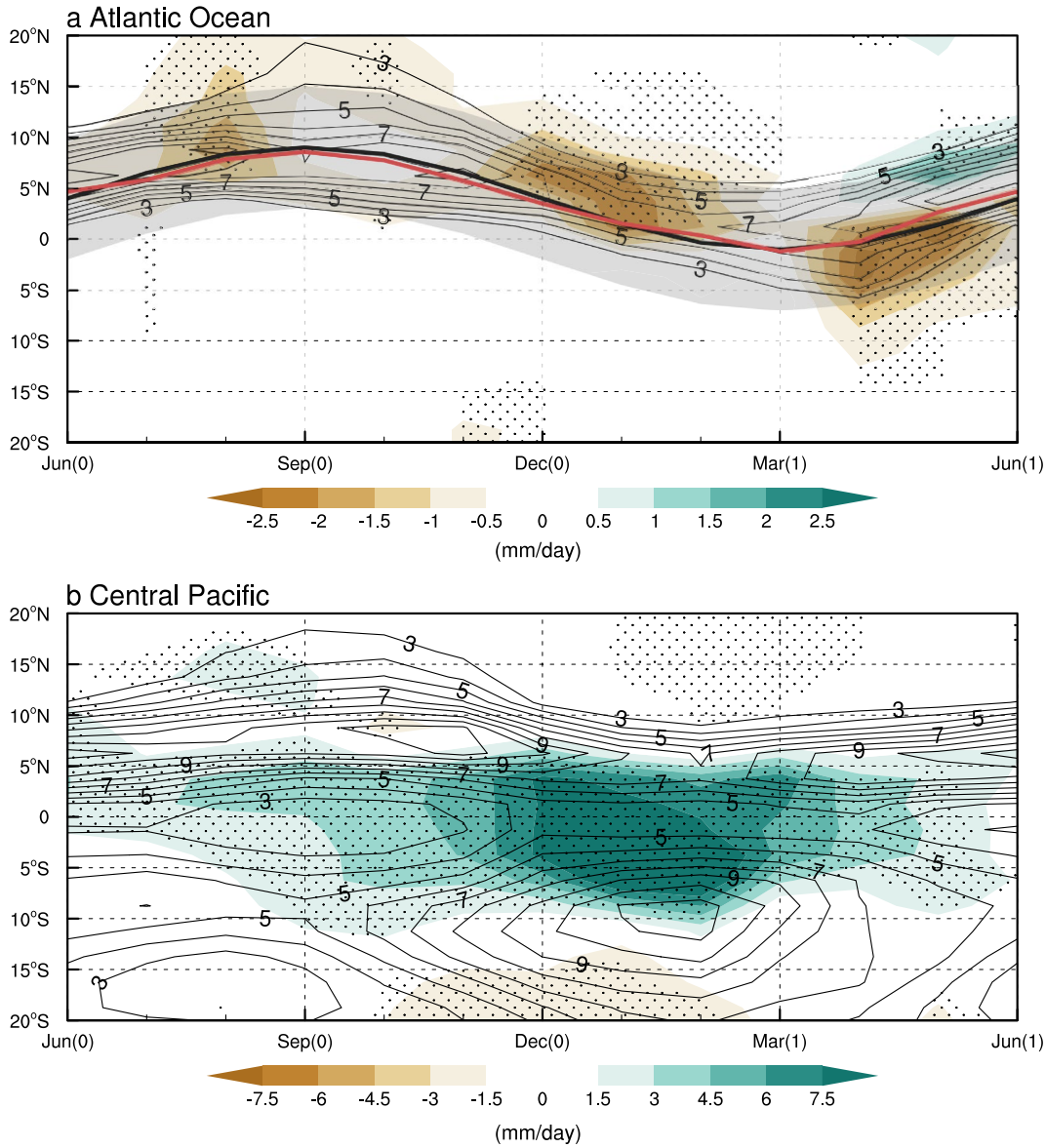

Figure 2. Latitude–time sections of climatological precipitation (contours; mm/day) and composite El Niño minus La Niña precipitation anomalies (shading; mm/day) averaged zonally over the (a) Atlantic (0°W–80°W) and (b) central Pacific (160°E–150°W). The red line in (a) denotes the climatological monthly Intertropical Convergence Zone (ITCZ) position and the black line denotes a sinusoidal fit to the ITCZ seasonal migration. The gray shading in (a) denotes the meridional range extending from 6° north of the climatological monthly ITCZ position to 6° south of it, roughly representing the main part of the ITCZ. The contour interval is 1 mm/day and contours smaller than 3 mm/day are omitted. Dots indicate anomalies that are statistically significant at the 95% confidence level.

into the landmass. Since the ITCZ over land is often irregular and detached from its oceanic counterparts (Waliser & Gautier, 1993), we here only focus on the marine ITCZ over the tropical Atlantic (black box in Figure S1). Despite some zonal asymmetry in its spatial pattern, the ITCZ over the tropical Atlantic migrates as a cohesive unit, reaching its northernmost latitudinal extent in boreal autumn and its southernmost latitudinal extent in boreal spring following the seasonal march of the solar insolation with about a quarter cycle lag (Gu & Adler, 2006; Hastenrath, 1991; Li & Philander, 1997; Mitchell & Wallace, 1992; Philander et al., 1996; S. P. Xie & Carton, 2004). To characterize the migration of the heaviest precipitation band back and forth, we provide a quantitative estimate of the climatological Atlantic ITCZ latitude throughout the annual cycle (red line in Figure 2a, $\bar{L}$). The seasonal ITCZ migration bears much resemblance to a sinusoidal pattern ($\bar{L}'(t) = 5\ \sin\left(\frac{\pi}{6} * t - \frac{5\pi}{6}\right) + 4$, where t is the

calendar month; black line in Figure 2a). The variance of the tropical Atlantic precipitation anomalies also displays a prominent seasonal displacement following a similar track (Figure S1).

In general, the ENSO-related precipitation anomalies in the tropical Atlantic are much smaller than the amplitude of the local seasonal cycle. During El Niño developing boreal summer to autumn, El Niño-related negative precipitation anomalies stay several degrees north of the equator (Figures 1b and 2a). In the following winter, the negative precipitation anomalies approach the equator. During El Niño decaying spring, the negative precipitation anomalies associated with El Niño events shift to the farthest south, located within 10°S–5°N. It is noted that relatively weak positive precipitation anomalies appear north of 5°N during the decaying spring, which is possibly associated with the tropical Atlantic meridional gradient of SST anomalies during El Niño events (e.g., Chiang et al., 2002; Nobre & Shukla, 1996; Saravanan & Chang, 2000). The positive north-south local SST gradient accompanies a northward cross-equatorial surface flow, which leads to convergence north of the equatorial Atlantic and therefore more precipitation here (e.g., Giannini et al., 2001). Despite that, the ENSO-related precipitation anomalies over the tropical Atlantic keep pace with the seasonal migration of the Atlantic ITCZ over the course of the seasonal cycle. This is in sharp contrast to the spatiotemporal features of the tropical precipitation over the central Pacific, where the precipitation variability is generally more meridionally stationary during El Niño events. The ITCZ in the central Pacific is composed of two regions of maximum precipitation straddling the equator (Figure 2b; e.g., Horel, 1982; Mitchell & Wallace, 1992). During ENSO episodes, the associated atmospheric deep convection alters the ITCZ structure over the Pacific basin, especially in boreal winter, exerting far-reaching impacts.

The above observational analyses show compelling evidence that the ENSO impact on Atlantic precipitation is strongly modulated by the local seasonal cycle. On this basis, we hereafter quantify the local seasonal cycle modulated ENSO-related precipitation over the tropical Atlantic. We define a seasonally adjusted region of the tropical Atlantic, the zonal extent of which is fixed within 0°W–90°W and the meridional extent is denoted by the gray shading within 6° north and south of the central latitude of the monthly climatological ITCZ in Figure 2a. As shown in Figure 3a, the tropical Atlantic precipitation averaged over the seasonally adjusted region corresponds well to ENSO variability temporally ($R = 0.68$, statistically significant at the 95% confidence level). Qualitative conclusions remain the same for slight changes in the meridional extent. This linear relationship is most prominent when the central-to-eastern Pacific experiences warmer than normal conditions, hinting at some El Niño/La Niña asymmetry (Figure 3b). Taking into account the modulation of the Atlantic ITCZ seasonal cycle, the ENSO-related tropical Atlantic precipitation anomalies can be well reproduced by reconstructing them using linear regression with ENSO conditions separately for each month (Figure 3c). In contrast, the reconstruction based on the monthly ENSO conditions without involving the seasonal cycle fails to reproduce the observed seasonal migration of the ENSO-related precipitation over the tropical Atlantic (Figure 3d). In this dynamic perspective, a robust year-round relationship is established between ENSO and precipitation anomalies over the tropical Atlantic by involving the local seasonal cycle.

4. Climate Model Simulations

Next, we examine the role of the Atlantic seasonal cycle in modulating ENSO impacts on tropical Atlantic precipitation in 50 CMIP6 pi-control simulations. We first assess the performance of CMIP6 models in reproducing ENSO seasonal synchronization behavior in terms of its preferred peaking month, which is a fundamental feature of ENSO (e.g., Chen & Jin, 2021; Stein et al., 2014). In the observations, ENSO SST anomaly variance is maximized in November–January. As shown in black circles in Figure 4a, 35 out of 50 CMIP6 models (see also Table S1) correctly simulate ENSO seasonal synchronization, simulating the ENSO peak phase in November–January. The ability of the models to simulate the climatological features of Atlantic precipitation is also evaluated. Despite continued model improvement, precipitation biases over the tropical Atlantic persist in state-of-the-art climate models (e.g., Richter & Tokinaga, 2020; Siongco et al., 2015). In most climate models, the seasonal swing of the Atlantic ITCZ is nearly symmetric with regard to the equator with excessive precipitation south of the equator during boreal spring (Figure S2; Dai, 2006; Richter & Tokinaga, 2020; Richter et al., 2014). To select the models that perform well over the tropical Atlantic region in terms of the seasonal variation in the intensity of the precipitation climatology as well as its seasonal migration, the pattern correlations of the latitude–time sections of the tropical Atlantic precipitation climatology with the observations are compared (Figure 4b

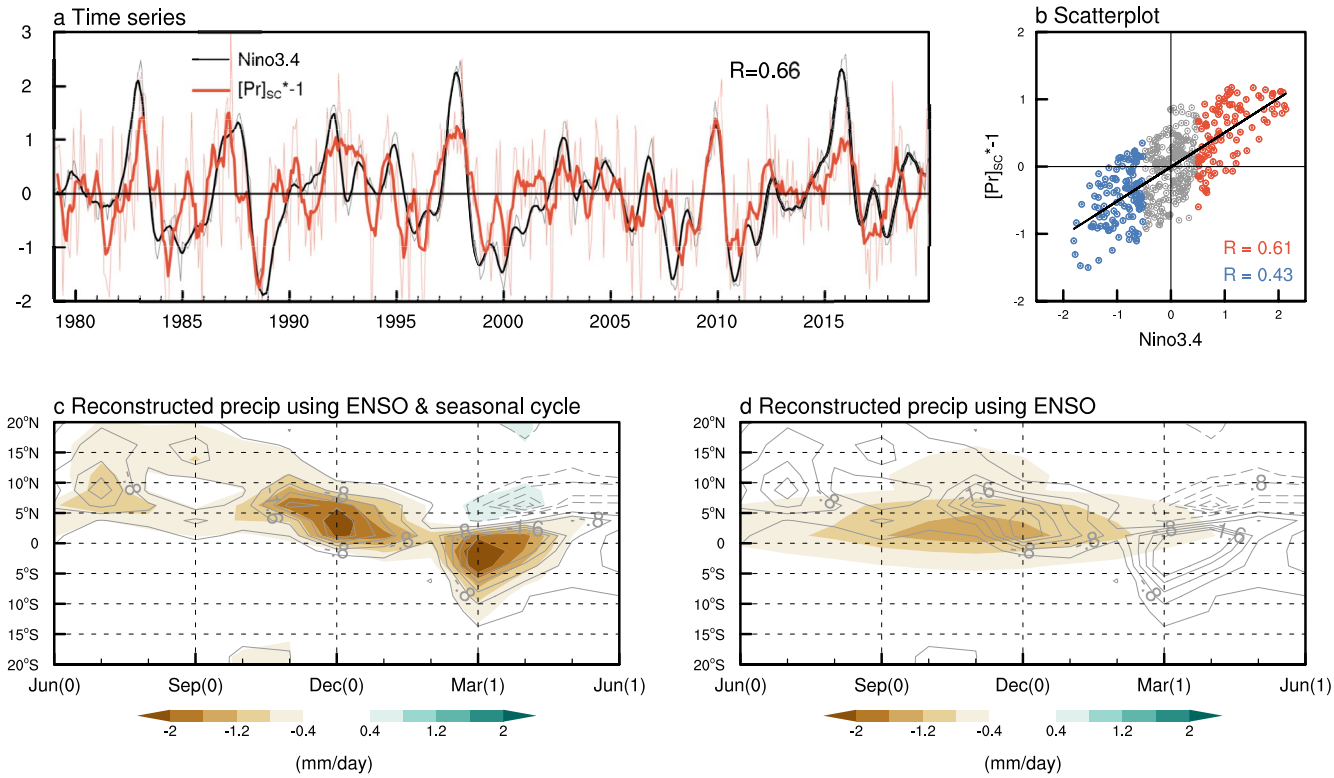

Figure 3. (a) Time series of running 6-month mean (thick line) and nonsmoothed (thin line) Niño3.4 index (black line) and the tropical Atlantic precipitation averaged over the seasonally adjusted region ($[Pr]_{SC}$, red line). The Atlantic precipitation is multiplied by a factor of − 1 for easy comparison. The correlation coefficient is also displayed. (b) Scatterplot of the Niño3.4 index and $[Pr]_{SC} * -1$. Red circles denote months with a Niño3.4 index greater than 0.5°C and blue circles denote months with a Niño3.4 index smaller than −0.5°C. (c, d) The linear fit is displayed together with the respective correlation coefficients for red and blue circles. (c, d) Latitude–time sections of the observed (contours; mm/day) and reconstructed (shading; mm/day) composite El Niño minus La Niña precipitation by considering (c) ENSO and the Atlantic seasonal cycle and (d) ENSO only. The contour interval in (c) and (d) is 0.4 mm/day. Correlation coefficients in (a) and (b) are calculated based on time series of running 6-month means for both the Niño3.4 index and the seasonal cycle modulated Atlantic precipitation anomalies to filter out high-frequency noise. Qualitatively, similar conclusions can be obtained using the unsmoothed data, although the correlation estimates are more conservative.

and Table S1). The models with correlation coefficients larger than 0.8 (Figure 4b and Table S1) are regarded as models that have the ability to realistically simulate the Atlantic seasonal cycle (Figure 4b).

Despite that many current climate models still struggle to accurately represent both the ENSO seasonal synchronization behavior and the Atlantic seasonal cycle, the role of the Atlantic seasonal cycle in modulating ENSO impacts over the tropical Atlantic precipitation is clearly evident (Figure 4c). That is, the state-of-the-art climate models are capable of simulating the local seasonal cycle modulated ENSO impact on the tropical Atlantic precipitation. The ENSO-related precipitation anomalies are located north of the equator during ENSO developing summer to autumn, approach the equator during the ENSO mature phase, and shift farthest south in the following spring. It is obvious that ENSO impacts on tropical Atlantic precipitation anomalies show an exaggeration of the latitudinal range, characterized by an excessive southward migration bias similar to that of the climatological Atlantic ITCZ in the all CMIP6 model ensemble mean. We next select six models that simulate both the correct ENSO seasonal synchronization behaviors and the climatological features of tropical Atlantic precipitation (Table S1). These models reproduce well the observed north-south asymmetry of the Atlantic ITCZ and the simulated ENSO impact on tropical Atlantic precipitation compares fairly well with observations (Figure 4d). Multimodel analyses indicate that the realistic representation of both ENSO variability and the local seasonal cycle is critical in simulating the ENSO-related regional climate anomalies, as suggested by previous studies (Stuecker et al., 2013, Zhang, Jin, et al., 2016, Zhang, Li, et al., 2016).

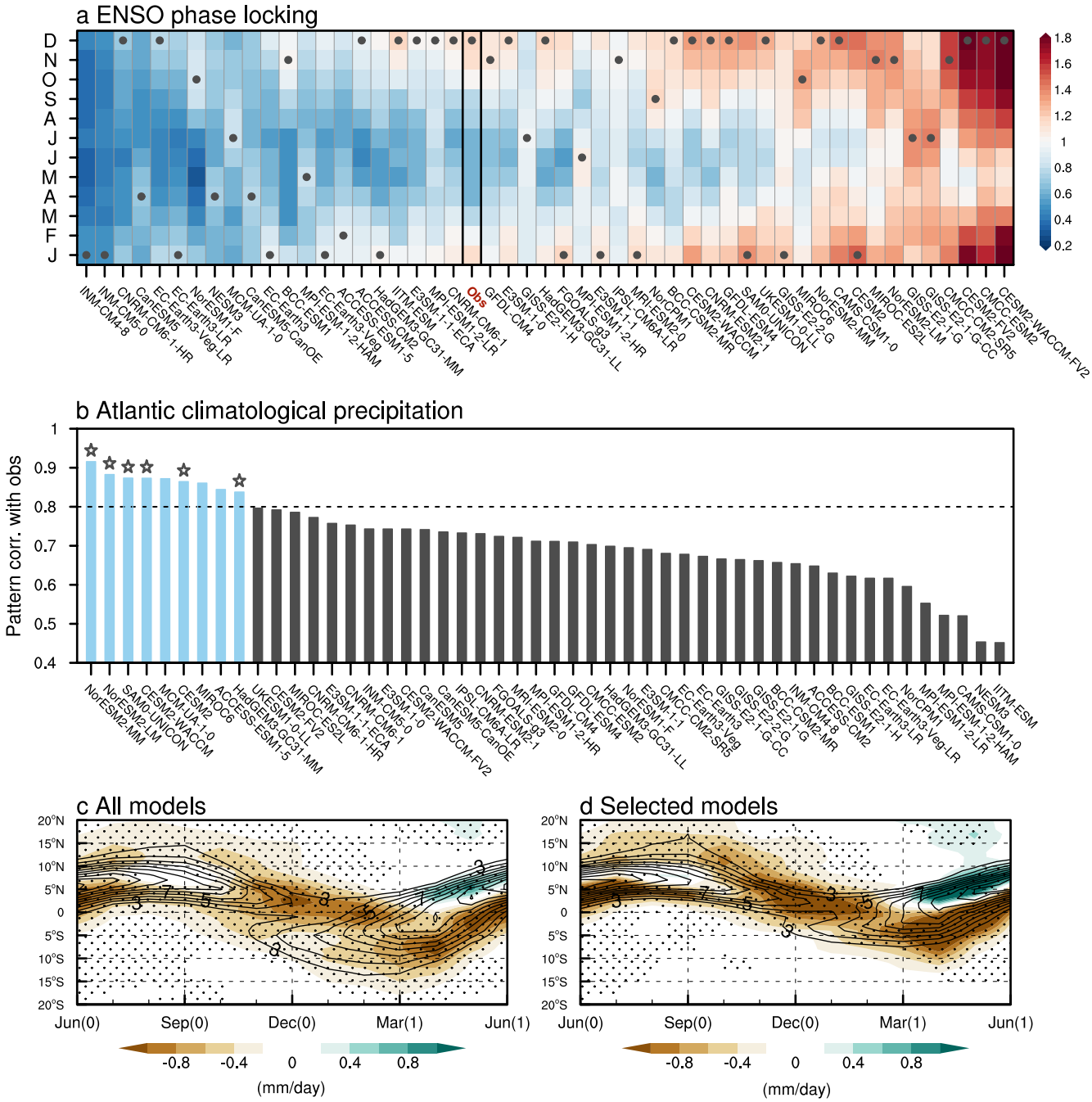

Figure 4. (a) Standard deviation of the Niño3.4 index stratified by calendar month for CMIP6 models, sorted by the strength of the annual mean standard deviation in ascending order. The observations are also shown for reference. The black dots indicate the calendar month with the maximum standard deviation for each model and the observations. The black box indicates the observation (obs). (b) Pattern correlations of the latitude–time sections of the tropical Atlantic precipitation climatology with the observations in a descending order. Blue bars indicate models with a correlation coefficient larger than 0.8 and gray bars indicate the remaining models. Asterisks indicate the models simulate both ENSO phase locking behavior in November–January and climatological features of tropical Atlantic precipitation well. (c, d) Ensemble mean of the latitude–time sections of climatological precipitation (contours; mm/day) and composite El Niño minus La Niña precipitation anomalies (shading; mm/day) averaged zonally over the Atlantic for (c) all models and (d) selected models that simulate both ENSO phase locking behavior and tropical Atlantic precipitation climatology. The contour interval in (c) and (d) is 1 mm/day and contours smaller than 3 mm/day are omitted. Dots in (c) and (d) indicate anomalies that are statistically significant at the 95% confidence level.

5. Summary and Discussion

Most previous studies investigating the ENSO teleconnection to tropical Atlantic climate variability have been primarily focused on the boreal spring season, based on the strong seasonality of the NTA SST response. In the precipitation field, the seasonal preference appears less apparent with an ENSO climate signal being detected within the tropical Atlantic region throughout the ENSO lifecycle. Here, we show that the Atlantic seasonal cycle strongly modulates the ENSO impact on tropical Atlantic precipitation in its meridional march. Taking into account this modulation by the local seasonal cycle, the full spatiotemporal characteristics of ENSO-related tropical Atlantic precipitation anomalies are quantified here, which turn out to be substantially larger than previously recognized.

The dynamic perspective on the ENSO impacts over the tropical Atlantic modulated by the local seasonal cycle we framed here enhances prospects for year-round seasonal prediction in the Atlantic sector. The advanced understanding of the potential predictability of Atlantic climate variability, especially in boreal summer and autumn, could also provide some clues to predicting the variability of Atlantic hurricane activity. Furthermore, we show that the realistic simulation of both ENSO variability (including its seasonal synchronization) and the Atlantic seasonal cycle is critical for realistically simulating the El Niño-related regional climate anomalies. Continued improvement of ENSO prediction and realistic representation of the Atlantic seasonal cycle are important for advancing seasonal climate prediction over the tropical Atlantic sector.

Data Availability Statement

The data used to reproduce the results of this paper are located at https://www.metoffice.gov.uk/hadobs/hadisst/data/download.html, https://psl.noaa.gov/data/gridded/data.cmap.html, https://www.esrl.noaa.gov/psd/data/gridded/data.ncep.reanalysis.html, and https://esgf-node.llnl.gov/projects/cmip6/.

Acknowledgments
This work was supported by the National Nature Science Foundation of China (42125501 and 42088101). M.F.S. was supported by NOAA's Climate Program Office's Modeling Analysis, Predictions, and Projections (MAPP) program, grant NA20OAR4310445. This is IPRC publication 1549 and SOEST contribution 11437.

References

Alexander, M. A., Bladé, I., Newman, M., Lanzante, J. R., Lau, N.-C., & Scott, J. D. (2002). The atmospheric bridge: The influence of ENSO teleconnections on air–sea interaction over the global oceans. *Journal of Climate*, *15*(16), 2205–2231. https://doi.org/10.1175/1520-0442(2002)015<2205:TABTIO>2.0.CO;2

Alexander, M., & Scott, J. (2002). The influence of ENSO on air–sea interaction in the Atlantic. *Geophysical Research Letters*, *29*(14), 1701. https://doi.org/10.1029/2001GL014347

Behera, S. K., Luo, J.-J., Masson, S., Rao, S. A., Sakuma, H., & Yamagata, T. (2006). A CGCM study on the interaction between IOD and ENSO. *Journal of Climate*, *19*(9), 1688–1705. https://doi.org/10.1175/JCLI3797.1

Bjerknes, J. (1969). Atmospheric teleconnections from the equatorial Pacific. *Monthly Weather Review*, *97*(3), 163–172. https://doi.org/10.1175/1520-0493(1969)097<0163:ATFTEP>2.3.CO;2

Cai, W., Wu, L., Lengaigne, M., Li, T., Mcgregor, S., Kug, J.-S., et al. (2019). Pantropical climate interactions. *Science*, *363*, eaav4236. https://doi.org/10.1126/science.aav4236

Chang, P., Fang, Y., Saravanan, R., Ji, L., & Seidel, H. (2006). The cause of the fragile relationship between the Pacific El Niño and the Atlantic Niño. *Nature*, *443*(7109), 324–328. https://doi.org/10.1038/nature05053

Chen, H.-C., & Jin, F. F. (2021). Simulations of ENSO phase-locking in CMIP5 and CMIP6. *Journal of Climate*, *34*(12), 5135–5149. https://doi.org/10.1175/JCLI-D-20-0874.1

Chiang, J. C., Kushnir, H. Y., & Giannini, A. (2002). Deconstructing Atlantic ITCZ variability: Influence of the local cross-equatorial SST gradient, and remote forcing from the eastern equatorial pacific. *Journal of Geophysical Research*, *107*(D1), 4004. https://doi.org/10.1029/2000JD000307

Covey, D. L., & Hastenrath, S. (1978). The Pacific El Niño phenomenon and the Atlantic circulation. *Monthly Weather Review*, *106*(9), 1280–1287. https://doi.org/10.1175/1520-0493(1978)106<1280:TPENPA>2.0.CO;2

Dai, A. (2006). Precipitation characteristics in eighteen coupled climate models. *Journal of Climate*, *19*(18), 4605–4630. https://doi.org/10.1175/JCLI3884.1

Dai, A., & Wigley, T. M. L. (2000). Global patterns of ENSO-induced precipitation. *Geophysical Research Letters*, *27*(9), 1283–1286. https://doi.org/10.1029/1999GL011140

Enfield, D. B., & Alfaro, E. J. (1999). The dependence of Caribbean rainfall on the interaction of the tropical Atlantic and Pacific Oceans. *Journal of Climate*, *12*(7), 2093–2103. https://doi.org/10.1175/1520-0442(1999)012<2093:TDOCRO>2.0.CO;2

Enfield, D. B., & Mayer, D. A. (1997). Tropical Atlantic sea surface temperature variability and its relation to El Niño–Southern Oscillation. *Journal of Geophysical Research*, *102*(C1), 929–945. https://doi.org/10.1029/96JC03296

Gadgil, S., & Guruprasad, A. (1990). An objective method for the identification of the intertropical convergence zone. *Journal of Climate*, *3*(5), 558–567. https://doi.org/10.1175/1520-0442(1990)003<0558:AOMFTI>2.0.CO;2

García-Serrano, J., Cassou, C., Douville, H., Giannini, A., & Doblas-Reyes, F. J. (2017). Revisiting the ENSO teleconnection to the tropical North Atlantic. *Journal of Climate*, *30*(17), 6945–6957.

Giannini, A., Chiang, J. C., Cane, M. A., Kushnir, Y., & Seager, R. (2001). The ENSO teleconnection to the tropical Atlantic Ocean: Contributions of the remote and local SSTs to rainfall variability in the tropical Americas. *Journal of Climate*, *14*(24), 4530–4544. https://doi.org/10.1175/1520-0442(2001)014<4530:TETTTT>2.0.CO;2

Gu, G., & Adler, R. F. (2006). Interannual rainfall variability in the tropical Atlantic region. *Journal of Geophysical Research*, *111*, D02106. https://doi.org/10.1029/2005JD005944

Hastenrath, S. (1991). Regional circulation systems. In *Climate dynamics of the tropics* (pp. 114–218). Dordrecht, The Netherlands: Springer. https://doi.org/10.1007/978-94-011-3156-8_6

Horel, J. D. (1982). On the annual cycle of the tropical Pacific atmosphere and ocean. *Monthly Weather Review*, *110*(12), 1863–1878. https://doi.org/10.1175/1520-0493(1982)110<1863:OTACOT>2.0.CO;2

Horel, J. D., & Wallace, J. M. (1981). Planetary-scale atmospheric phenomena associated with the Southern Oscillation. *Monthly Weather Review*, *109*(4), 813–829. https://doi.org/10.1175/1520-0493(1981)109<0813:PSAPAW>2.0.CO;2

Jin, F.-F. (1997). An equatorial ocean recharge paradigm for ENSO. Part I: Conceptual model. *Journal of the Atmospheric Sciences*, *54*(7), 811–829. https://doi.org/10.1175/1520-0469(1997)054<0811:AEORPF>2.0.CO;2

Kalnay, E., Kanamitsu, M., Kistler, R., Collins, W., Deaven, D., Gandin, L., et al. (1996). The NCEP/NCAR 40-year reanalysis project. *Bulletin of the American Meteorological Society*, *77*(3), 437–471. https://doi.org/10.1175/1520-0477(1996)077<0437:TNYRP>2.0.CO;2

Kim, S., Son, H.-Y., & Kug, J.-S. (2018). Relative roles of equatorial central Pacific and western North Pacific precipitation anomalies in ENSO teleconnection over the North Pacific. *Climate Dynamics*, *51*(11–12), 4345–4355. https://doi.org/10.1007/s00382-017-3779-6

Klein, S. A., Soden, B. J., & Lau, N. C. (1999). Remote sea surface temperature variations during ENSO: Evidence for a tropical atmospheric bridge. *Journal of Climate*, *12*(4), 917–932. https://doi.org/10.1175/1520-0442(1999)012<0917:RSSTVD>2.0.CO;2

Kushnir, Y., Robinson, W. A., Chang, P., & Robertson, A. W. (2006). The physical basis for predicting Atlantic sector seasonal-to-interannual climate variability. *Journal of Climate*, *19*(23), 5949–5970. https://doi.org/10.1175/JCLI3943.1

Lintner, B. R., & Chiang, J. C. H. (2007). Adjustment of the remote tropical climate to El Niño conditions. *Journal of Climate*, *20*(11), 2544–2557. https://doi.org/10.1175/JCLI4138.1

Li, T., & Philander, S. G. H. (1997). On the seasonal cycle of the equatorial Atlantic Ocean. *Journal of Climate*, *10*(4), 813–817. https://doi.org/10.1175/1520-0442(1997)010<0813:OTSCOT>2.0.CO;2

Livezey, R. E., Masutani, M., Leetmaa, A., Rui, H., Ji, M., & Kumar, A. (1997). Teleconnective response of the Pacific–North American Region atmosphere to large central equatorial pacific SST anomalies. *Journal of Climate*, *10*(8), 1787–1820. https://doi.org/10.1175/1520-0442(1997)010<1787:TROTPN>2.0.CO;2

McPhaden, M. J., Zebiak, S. E., & Glantz, M. H. (2006). ENSO as an integrating concept in Earth science. *Science*, *314*(5806), 1740–1745. https://doi.org/10.1126/science.1132588

Mitchell, T. P., & Wallace, J. M. (1992). The annual cycle in equatorial convection and sea surface temperature. *Journal of Climate*, *5*(10), 1140–1156. https://doi.org/10.1175/1520-0442(1992)005<1140:TACIEC>2.0.CO;2

Münnich, M., & Neelin, J. D. (2005). Seasonal influence of ENSO on the Atlantic ITCZ and equatorial South America. *Geophysical Research Letters*, *32*, L21709. https://doi.org/10.1029/2005GL023900

Neelin, J. D., Battisti, D. S., Hirst, A. C., Jin, F. F., Wakata, Y., Yamagata, T., & Zebiak, S. E. (1998). ENSO theory. *Journal of Geophysical Research*, *103*(C7), 14261–14290. https://doi.org/10.1029/97JC03424

Nobre, P., & Shukla, J. (1996). Variations of sea surface temperature, wind stress, and rainfall over the tropical Atlantic and South America. *Journal of Climate*, *9*(10), 2464–2479. https://doi.org/10.1175/1520-0442(1996)009<2464:VOSSTW>2.0.CO;2

Philander, S. G. H. (1990). *The Southern Oscillation: Variability of the tropical atmosphere. El Niño, La Niña, and the Southern Oscillation* (pp. 9–157). Elsevier.

Philander, S. G. H., Gu, D., Lambert, G., Li, T., Halpern, D., Lau, N. C., & Pacanowski, R. C. (1996). Why the ITCZ is mostly north of the equator. *Journal of Climate*, *9*(12), 2958–2972. https://doi.org/10.1175/1520-0442(1996)009<2958:WTIIMN>2.0.CO;2

Rasmusson, E. M., & Carpenter, T. H. (1982). Variations in tropical sea surface temperature and surface wind fields associated with the Southern Oscillation/El Niño. *Monthly Weather Review*, *110*(5), 354–384. https://doi.org/10.1175/1520-0493(1982)110<0354:VITSST>2.0.CO;2

Rayner, N. A. A., Parker, D. E., Horton, E. B., Folland, C. K., Alexander, L. V., Rowell, D. P., & Kaplan, A. (2003). Global analyses of sea surface temperature, sea ice, and night marine air temperature since the late nineteenth century. *Journal of Geophysical Research*, *108*(D14), 4407. https://doi.org/10.1029/2002JD002670

Reason, C. J. C., Allan, R. J., Lindesay, J. A., & Ansell, T. J. (2000). ENSO and climatic signals across the Indian Ocean basin in the global context: Part I, Interannual composite patterns. *International Journal of Climatology*, *20*(11), 1285–1327. https://doi.org/10.1002/1097-0088(200009)20:11<1285::AID-JOC536>3.0.CO;2-R

Richter, I., & Tokinaga, H. (2020). An overview of the performance of CMIP6 models in the tropical Atlantic: Mean state, variability, and remote impacts. *Climate Dynamics*, *55*(9–10), 2579–2601. https://doi.org/10.1007/s00382-020-05409-w

Richter, I., Xie, S.-P., Behera, S. K., Doi, T., & Masumoto, Y. (2014). Equatorial Atlantic variability and its relation to mean state biases in CMIP5. *Climate Dynamics*, *42*(1–2), 171–188. https://doi.org/10.1007/s00382-012-1624-5

Ropelewski, C. F., & Halpert, M. S. (1987). Global and regional scale precipitation patterns associated with the El Niño/Southern Oscillation. *Monthly Weather Review*, *115*(8), 1606–1626. https://doi.org/10.1175/1520-0493(1987)115<1606:GARSPP>2.0.CO;2

Saravanan, R., & Chang, P. (2000). Interaction between tropical Atlantic variability and El Niño–Southern oscillation. *Journal of Climate*, *13*(13), 2177–2194. https://doi.org/10.1175/1520-0442(2000)013<2177:IBTAVA>2.0.CO;2

Sasaki, W., Doi, T., Richards, K. J., & Masumoto, Y. (2015). The influence of ENSO on the equatorial Atlantic precipitation through the Walker circulation in a CGCM. *Climate Dynamics*, *44*(1–2), 191–202. https://doi.org/10.1007/s00382-014-2133-5

Siongco, A. C., Hohenegger, C., & Stevens, B. (2015). The Atlantic ITCZ bias in CMIP5 models. *Climate Dynamics*, *45*(5–6), 1169–1180. https://doi.org/10.1007/s00382-014-2366-3

Stein, K., Timmermann, A., Schneider, N., Jin, F.-F., & Stuecker, M. F. (2014). ENSO seasonal synchronization theory. *Journal of Climate*, *27*(14), 5285–5310. https://doi.org/10.1175/JCLI-D-13-00525.1

Stuecker, M. F., Timmermann, A., Jin, F.-F., Chikamoto, Y., Zhang, W., Wittenberg, A. T., et al. (2017). Revisiting ENSO/Indian Ocean dipole phase relationships. *Geophysical Research Letters*, *44*, 2481–2492. https://doi.org/10.1002/2016GL072308

Stuecker, M. F., Timmermann, A., Jin, F.-F., McGregor, S., & Ren, H.-L. (2013). A combination mode of the annual cycle and the El Niño/Southern Oscillation. *Nature Geoscience*, *6*(7), 540–544. https://doi.org/10.1038/ngeo1826

Waliser, D. E., & Gautier, C. (1993). A satellite-derived climatology of the ITCZ. *Journal of Climate*, *6*, 2162–2174. https://doi.org/10.1175/1520-0442(1993)006<2162:ASDCOT>2.0.CO;2

Wallace, J. M., Rasmusson, E. M., Mitchell, T. P., Kousky, V. E., Sarachik, E. S., & Von Storch, H. (1998). On the structure and evolution of ENSO-related climate variability in the tropical Pacific: Lessons from TOGA. *Journal of Geophysical Research*, *103*(C7), 14241–14259. https://doi.org/10.1029/97JC02905

Wang, H., & Fu, R. (2000). Winter Monthly Mean Atmospheric Anomalies over the North Pacific and North America Associated with El Niño SSTs. *Journal of Climate*, *13*(19), 3435–3447. https://doi.org/10.1175/1520-0442(2000)013<3435:WMMAAO>2.0.CO;2

Wyrtki, K. (1975). El Niño—The dynamic response of the equatorial Pacific Ocean to atmospheric forcing. *Journal of Physical Oceanography*, *5*(4), 572–584. https://doi.org/10.1175/1520-0485(1975)005<0572:ENTDRO>2.0.CO;2

Xie, P., & Arkin, P. A. (1996). Analyses of global monthly precipitation using gauge observations, satellite estimates, and numerical model predictions. *Journal of Climate*, *9*(4), 840–858. https://doi.org/10.1175/1520-0442(1996)009<0840:AOGMPU>2.0.CO;2

Xie, S.-P., & Carton, J. A. (2004). Tropical Atlantic variability: Patterns, mechanisms, and impacts. Earth's climate: The ocean–atmosphere interaction. *Geophysical Monograph Series*, 147, 121–142. https://doi.org/10.1029/147GM07

Yang, J., Liu, Q., Xie, S. P., Liu, Z., & Wu, L. (2007). Impact of the Indian Ocean SST basin mode on the Asian summer monsoon. *Geophysical Research Letters*, *34*, L02708. https://doi.org/10.1029/2006GL028571

Yun, K. S., Timmermann, A., & Stuecker, M. F. (2021). Synchronized spatial shifts of Hadley and Walker circulations. *Earth System Dynamics*, *12*(1), 121–132. https://doi.org/10.5194/esd-12-121-2021

Zhang, W., Jin, F.-F., Stuecker, M. F., Wittenberg, A. T., Timmermann, A., Ren, H. L., et al. (2016). Unraveling El Niño's impact on the East Asian monsoon and Yangtze River summer flooding. *Geophysical Research Letters*, *43*, 11–375. https://doi.org/10.1002/2016GL071190

Zhang, W., Li, H., Stuecker, M. F., Jin, F. F., & Turner, A. G. (2016). A new understanding of El Niño's impact over East Asia: Dominance of the ENSO combination mode. *Journal of Climate*, *29*(12), 4347–4359. https://doi.org/10.1175/JCLI-D-15-0104.1